ISSN 1392–1320 MATERIALS SCIENCE (MEDŽIAGOTYRA). Vol. 15, No. 1. 2009

Investigation of Silver Nanoparticles Formation Kinetics During Reduction of Silver Nitrate with Sodium Citrate

Asta ŠILEIKAITĖ[1*], Judita PUIŠO[1,2], Igoris PROSYČEVAS[1], Sigitas TAMULEVIČIUS[1,2]

[1]*Institute of Physical Electronics of Kaunas University of Technology, Savanorių av. 271, Kaunas LT-50131, Lithuania*
[2]*Department of Physics, Kaunas University of Technology, Studentų str. 50, Kaunas LT-51368, Lithuania*

Received 11 September 2008; accepted 06 October 2008

In the present research the formation kinetics of silver nanoparticles during synthesis of silver colloidal solution (silver nitrate reduction with sodium citrate) was investigated. The formation of silver nanoparticles was monitored with optical spectrophotometer measuring optical absorbance spectra. Optical spectra were taken after the reducing agent was introduced to the silver salt solution (1, 2, 5, 10, 15, 20, 25, 30, 45, 60, 120 min). Approximating spectra with Gaussian function statistical parameters (surface plasmon resonance position, full width at half maximum, intensity) were found. Theoretical calculations employing software "MiePlot v. 3.4" which is based on Mie scattering theory was done. Comparison of theoretical and experimental results has shown that the size of nanoparticles present in the solution varies in the range of 45 nm – 80 nm. Scanning electron microscope was employed for direct determination of the nanoparticle size. The time stability of colloidal solution was investigated.
Keywords: silver nanoparticles, formation kinetics, surface plasmon resonance, colloidal stability.

1. INTRODUCTION

There is a huge interest in metal nanoparticles because of their unexpected physical and chemical properties shown at nanoscale. Metal nanoparticles could be key elements for applications in optics and electronics mainly because of the quantized motion of the collectively excited conduction electrons, the size dependent 'surface plasmons', which results in extraordinary large electromagnetic field enhancements, upon interaction with an incoming electromagnetic field [1]. The plasmon resonance is strongly dependent on the size, shape, dielectric properties of the particle and its surroundings. Changing the synthesis routes, particles with different shape (spheres [2], rods [3], triangulars [4]) and size (from few nanometers to hundreds) in different media (water, alcohols, polymers) can be formed. There is a wide variety of silver nanoparticles preparation techniques. The most popular preparation methods are chemical reduction using different reducing agents [5 – 7], photochemical preparation [8], radiolysis [9].The main problem of the these methods is stability of the formed nanoparticle systems and sometimes difficult handling of the synthesis (e. g. radiolysis). Other possibility to obtain stable nanoparticle systems is to use vacuum deposition and lithographic techniques.

The key feature in application of silver nanoparticles is the stability of formed system. Until now stable systems could be obtained via immobilization of nanoparticles on substrates. This can be achieved via electron beam lithography (EBL) or vacuum deposition of metal. Recently it was announced about the stable colloidal system of triangular plates of silver which was successfully used for biosensor applications [4].

Silver nanoparticles are widely used in surface enhanced Raman scattering (SERS) spectroscopy because of high local field enhancement factor. For this purpose, silver nanoparticles can be dispersed in solution [10] or formed on the substrates [11]. Also silver nanoparticles can be used for modification of polymer based diffraction gratings [12] which further can be used in grating light reflection spectroscopy for sensing [13].

In this work we present the investigation of silver nanoparticles formation kinetics during the chemical reduction of silver nitrate with sodium citrate. The tasks of this work were to find the optimal time of synthesis duration and investigate the time stability of formed colloidal solution.

2. EXPERIMENTAL

2.1. Formation of silver colloid

The silver colloid was prepared by chemical reduction method according to the description of Lee and Meisel [14]. Silver nitrate $AgNO_3$ (Sigma Aldrich, UK) and trisodium citrate $C_6H_5O_7Na_3$ (Sigma Aldrich, UK) of analytical grade purity, were used as starting materials without further purification.

All solutions of reacting materials were prepared in distilled water. In typical experiment 500 ml of $1 \cdot 10^{-3}$ M $AgNO_3$ was heated to boiling. To this solution 5 ml of 1 % trisodium citrate was added drop by drop. During the process solution was mixed vigorously. The mechanism of silver nanoparticles formation reaction can be found in [15]. After 2 hours heating the solution was removed from the heating element and stirred until cooled to room temperature.

2.2. Investigation of formation kinetics

In order to determine the kinetics of formation of silver nanoparticles, the UV-VIS spectra were measured

*Corresponding author. Tel. +370-37-313432, fax. +370-37-314423.
E-mail address: *asta.sileikaite@stud.ktu.lt* (A. Šileikaitė)

during the boiling process after the addition of reducing agent ($C_6H_5O_7Na_3$). Measurement of transmission directly yields the extinction of light, which is the evidence of the formation of silver nanoparticles. At the beginning of the boiling spectra, were taken after 1, 2, 5 min to find when the formation of silver nanoparticles starts. Later, when the start of formation was reached, the spectra were measured after each 10 min – 15 min has passed up to the 60 min. After one hour has passed spectra were taken after each half of an hour while 120 min after the boiling start was reached.

2.3. Analytical techniques

The UV-VIS light spectrophotometer (Avantes 2048) was used for determination of silver nanoparticles formation measuring optical absorbance spectra. This spectrophotometer is composed of deuterium halogen light source (AvaLight DHc) and spectrometer (Avaspec-2048) with a detection system of 2048 pixel charge coupled device (CCD). It is possible to use the spectrometer in region from 192 nm to 1100 nm with the resolution of 1.4 nm. The statistical parameters of absorbance spectra were determined approximating data with Gaussian distribution. The approximation was done employing "IgorPro 6.0" software [16].

Colloidal particles were also imaged with a field emission scanning electron microscope (SEM) Hitachi S-4800. It employs a conventional semi-in-lens design for large sample accommodation while achieving ultra-high resolution (UHR) comparable to performance only available with in-lens UHR SEMs. A guaranteed resolution of 2.0 nm at 1 kV for low voltage applications is attainable. Using deacceleration function it is possible to use 0.1 kV accelerating voltage. Advanced dry vacuum system is designed including Ion pumps (IP) and Turbo Molecular Pump (TMP). The sample was prepared by dropping initial and four times diluted and sonicated (for 1 minute) colloidal solution on a clean silicon wafer and drying it in vacuum. The micrographs of nanoparticles were analysed with "ImageJ 1.34s" [17] software.

3. RESULTS AND DISCUSSIONS

3.1. Optical measurements

The absorbance of silver colloidal solution was measured after the solution of $AgNO_3$ began to boil and reducing agent (1 % sodium citrate) was added. The spectra were taken after 1, 2, 5 and 10 minutes but there was no changes observed in that part of spectra where characteristic silver absorbance peak has to be observed (see Fig. 1, a). After 20 min of boiling small absorption band around 400 nm was observed. The peak was low in intensity and very broad. According to literature broad peaks in the beginning of formation is attributed to very small particles (seeds) [18]. With increase of time the absorption band has increased with intensity also (see Fig. 1, a). One can see in the spectra the minima at ~320 nm, which corresponds to a minimum in the imaginary part of the refractive index ($n_{Im} \sim 0.4$ for bulk silver). The depth of this minimum depends on the particle radius [19]. After 25 minutes of boiling have passed, the absorbance has increased and a shoulder at 350 nm appeared. The exact nature of this shoulder is not fully understood, but it is a part of plasmon resonance and its appearance is predicted by theoretical calculations based on Mie formulations [20]. The increase of absorbance is observed when the rate of silver nanoparticles formation has increased and more particles are formed during the same time. With the increase in absorbance, the background line is also shifted to about 1 a.u. in the absorbance spectra.

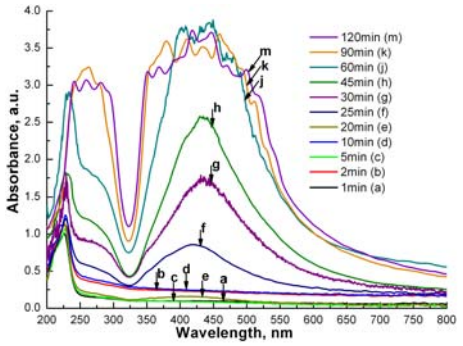

a

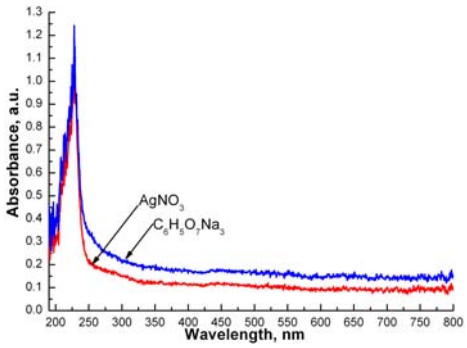

b

Fig. 1. UV-VIS spectra: a – evolution of absorbance spectra of silver colloidal solution; b – of initial components of silver colloidal solution

One can see in Fig. 1, a, that close to the silver absorption band the absorption at shorter wavelengths appears. This absorption could be attributed to the initial solutions: sodium citrate ($C_6H_5O_7Na_3$) and silver nitrate ($AgNO_3$). The absorbance spectra of these solutions are presented in Fig. 1, b. At longer times of boiling the peak in shorter wavelengths becomes broader and red-shifted from 225 nm to 275 nm. This broadening could be attributed to the appearance of clusters of silver ions Ag_2^+ in the solution [21]. Increasing time of boiling the absorbance spectrum becomes more intensive due to continuous formation of nanoparticles. The maximum absorbance that can be measured with the spectrophotometer is obtained at 60 min after the start of boiling. The boiling was continued to 120 min to find whether silver nanoparticles aggregate to bigger clusters or form clusters of other geometries. In this case the shifting of the peak could be observed. One could see that the peak at longer boiling times becomes broader; it means that the size distribution of particles becomes wider, but the position of the peak is stable (varies in few nanometer range). The spikes on the

absorbance peak (Fig. 1, a) are due to averaging of the resulting spectrum. There is no point to discuss about the increase of absorbance (when the boiling was continued for 60 minutes and longer) which directly yields to the quantity of silver nanoparticles, because the limits of detection of spectrophotometer were reached.

3.2. Statistical analysis (Comparison of theoretical and experimental results)

To determine the particle size in the solutions we performed several calculations with computer simulation program "MiePlot v. 3.4" [22], which is based on Mie scattering theory. The procedure was performed as described in [15].

These calculations have one disadvantage that it can be applied only in the case of spherical particles. As one can see, in the absorbance spectra there is only one peak (we do not take in mind the peak at shorter wavelengths because it is originated from the initial compounds), so we can conclude that our particles are spherical. From the absorbance spectra we can determine size of the particles comparing with the calculated one using Mie theory. One can find useful information analysing the optical spectra. The change in absorbance shows change of absorbing species in a solution, in our case – variations of the quantity of silver nanoparticles. Full width at half maximum gives information about the particle size distribution. The position of the peak directly depends on the size of nanoparticles [15]. As the size of particle increases, the SPR position shifts to longer wavelengths (red shift). In order to find all these parameters we have employed "IgorPro 6.0" software. Gaussian approximation was performed to find statistical parameters (full width at half maximum – FWHM, SPR position, absorbance intensity). Results of the statistical analysis of experimental data are listed in Table 1. The determination of SPR position (approximation with Gaussian function) for the last experimental points (90 min and 120 min) was not achieved because the signal was saturated. At this case all parameters (SPR position, FWHM and absorbance intensity) were determined by hand (evaluating the height of the peak and middle value at the FWHM).

Table 1. Statistical parameters of Ag colloidal solution

Boiling time, min	SPR position, nm	FWHM, nm	Absorbance, a.u.
20	406.77 ±0.25	96.55 ±0.67	0.09 ±0.0005
25	423.24 ±0.28	68.82 ±0.69	0.53 ±0.004
30	423.66 ±0.24	61.18 ±0.64	1.37 ±0.01
45	438.49 ±0.37	68.44 ±0.75	1.83 ±0.02
60	439.79 ±0.44	84.43 ±1.34	2.99 ±0.04
90	433.00 ±2.78	177.34 ±1.40	2.29 ±0.01
120	422.64 ±2.78	189.07 ±1.40	2.64 ±0.01

Graphical illustration of the statistical parameters determined from the experiment and theoretical calculations is shown in Figs. 2 – 4.

One can see the SPR position dependence on boiling time in Fig. 2, a. The dependence can be approximated with an exponential function. The data fits exponential function $y(x) = 441.06 - 191.66 \exp(-0.09x)$ with $R^2 = 96$ %. From the theoretical considerations (see Fig. 2, b) one could see that the position of the SPR is dependent on the size of the particles in a solution. Theoretical data fits linear function $y(x) = 362.74 + 0.95x$ with $R^2 = 99.7$ %. The SPR position in experimental data changes from 406.77 nm to 439.79 nm. Comparing the same region with the theoretical data gives the size of the particles varying from 45 nm to 80 nm at different stages of boiling.

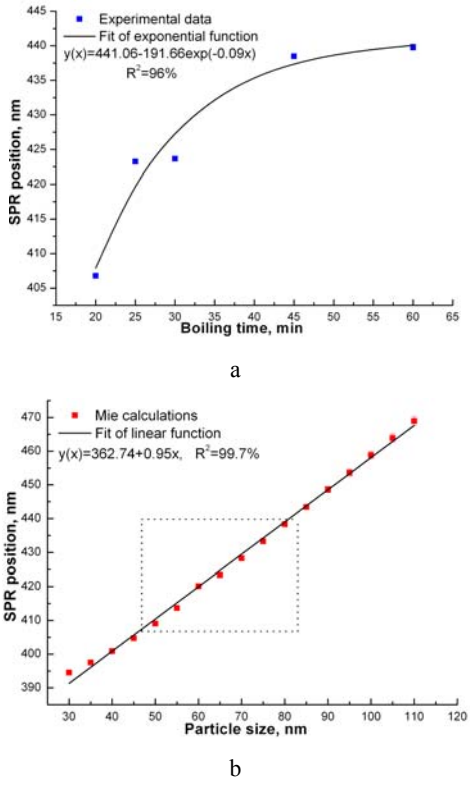

Fig. 2. SPR position dependence: a – on boiling time (determined from experimental data), b – on particle size (calculated using Mie theory), dotted rectangular shows region of interest – SPR variation region in experimental data

Full width at half maximum can be useful to find size distribution of the particles in a solution. The broader is the peak, the broader is the size distribution of the particles. Theoretical model suggests that with the increase of the particle size the FWHM is also increasing (in our calculations from 10 nm to 130 nm when the size of particle is 30 nm and 110 nm respectively), see Fig. 3, b. It can be explained by the optical processes. While the size of the particle is much smaller than the optical wavelength only absorbance can occur (5 nm – 20 nm). With the increase of particle size scattering becomes dominant and the peak becomes broader. The FWHM is increasing exponentially, this was determined approximating data with exponential function $y = 5.79 \exp(0.03x)$, $R^2 = 97$ %. One can see in Fig. 3, a, that experimental data has a similar tendency as theoretical. The data was approximated with two exponential functions: $y = 231.77 \exp(-0.05x)$, $R^2 = 92.76$ % (period 20 min – 30 min), and $y = 37.16 \exp(0.02x)$, $R^2 = 89.63$ %

(period 45 min –120 min) As it was mentioned above, the size of nanoparticles in a solution is predicted to be between 45 nm and 80 nm. One could predict from the theoretical graph of FWHM that the experimental FWHM should vary between 22 nm and 66 nm. This prediction was not observed in the experimental data (see Fig. 3, a). This could be explained by the overlapping of absorbance peaks originating from different sizes of the particles. The software "MiePlot" allows calculations of the particle size with standard deviation of 20 %. We can suppose that there is higher polidispersity than 20 % from the middle size value.

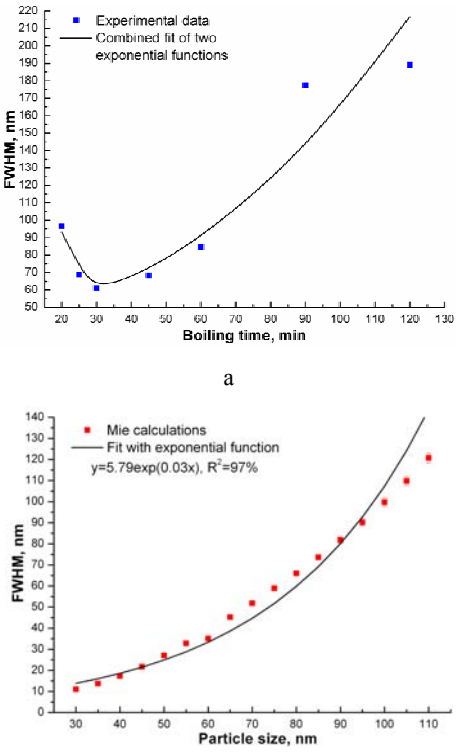

Fig. 3. FWHM of SPR peak: a – dependence on boiling time, b – dependence on particle size (theoretical calculations)

One could have noticed that during the process of boiling the intensity of absorbance has increased dramatically from the initial to the final steps (see Fig. 1, a). The dependence of the absorbance intensity on the particle size was determined from the Mie theory (see Fig. 4, b). From the calculated results one could see that with the increase of particle size the absorbance intensity decreases and the peak broadens (this can be seen in Fig. 4, b). The decrease of absorbance intensity has exponential dependence ($y = 26.17\exp(-0.02x)$, $R^2 = 99$ %). This could be explained having in mind the expression of extinction coefficient [15] that is proportional to reciprocal square of the particle size. The experimental data (see Fig. 4, a) shows that the intensity of absorbance has increased all the time until the boiling was performed for 60 min. Later (after 90 min and 120 min) the absorbance intensity still increased, but the higher background was observed. In all cases the background was subtracted. That is why the determined intensity is lower than the observed one in earlier steps of boiling. As these last points were not included in the approximation, we have found that the experimental data obeys a logarithmic function $y = 2.51\ln(x) - 7.44$, $R^2 = 96.3$ %. Comparing theoretical and experimental results one could conclude that in our experiment increase of the absorbance was influenced by the decrease of the size of the nanoparticles. On the other hand, the theoretical predictions analysed above contradict to this statement. It is more likely that the increase of absorbance is influenced by the increase of the amount of absorbing species in a solution (it is known from Bugert-Lamber-Beer law ($A = \alpha cl$, here A – absorbance in a.u., α – molar extinction coefficient in $M^{-1}\cdot cm^{-1}$, c – concentration of the absorbing species in M/l, l – thickness of the sample in cm).

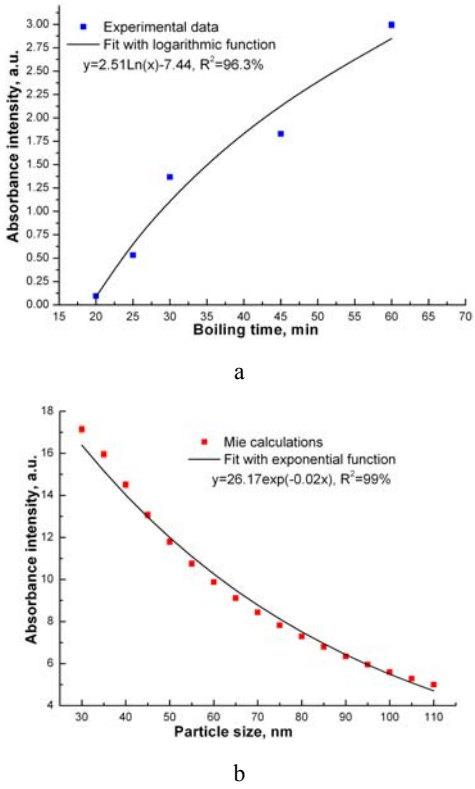

Fig. 4. Absorbance intensity dependence on: a – boiling time (experimental), b – particle size (theory)

3.3 Size determination with SEM

To determine the particle shape and size we have dispersed a drop of colloidal solution on clean silicon, dried it in ambient conditions and imaged with SEM. We have observed that particles tend to stick on the surface and form agglomerates (see Fig. 6, a), so it is a big challenge to determine the real shape of nanoparticles. In order to reduce agglomeration we have diluted (4 times) the colloidal solution and dried the drop of it on silicon in vacuum. This time the rate of agglomeration was lower and one could distinguish that the particles in a solution are not only spherical (see Fig. 6, b). One can see that there is spherical, hexagonal and elongated nanoparticles, which also vary in size. From the SEM micrographs of the colloidal nanoparticles (diluted) dispersed on a silicon wafer (Fig. 6, b) one can see that the nanoparticles vary in shape (spheres, hexagons, nanorods) and in size. But we should also stress that spherical particles dominate (see

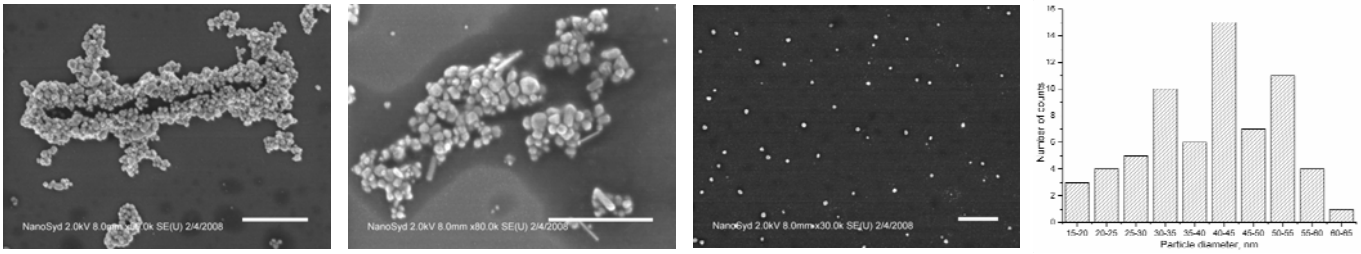

a b c d

Fig. 5. SEM micrographs of colloidal solution dried on silicon: a – initial solution, b – diluted solution, c – micrograph used for determination of size distribution, d – particle size distribution. Scale bar – 500 nm.

Fig. 7, a). Using the "ImageJ 1.34s" software we have determined the particle size distribution (Fig. 7, b). Employing "ImageJ 1.34s" the area of nanoparticles was determined in pixels. Pixels were converted to nanometers applying scale on the picture. The diameter of nanoparticles was calculated with Microsoft Excel, having in mind that area of the sphere is:

$$S = \frac{\pi d^2}{4}, \quad (1)$$

here S – is the area in m^2, d – is the diameter of a particle in m.We have obtained that the particles were varying in diameter from 3.2 nm to 60.4 nm (see Fig. 5, d). This could explain a broad absorption peak in the absorption spectra of the colloid (see Fig. 1, a). If we would neglect the smallest particles (up to 10 nm in diameter) then the maximum of the distribution would be for the range between 40 nm and 45 nm sized particles. The fit of the optical absorption spectra with Mie theory reveals that the spectral maximum position corresponds to particles between 45 nm and 80 nm size. The size of the particles calculated from the optical spectra (see Fig. 2, b) thus correlates roughly with those determined from the SEM pictures (see Fig. 5, d). This may be influenced by the uncertainties from optical measurements (particles are not only spherical, while the theoretical calculations are suitable only for spherical ones). Also some uncertainty was introduced in size determination from the SEM picture.

3.4. Stability of colloidal solution

There are many factors influencing the stability of a colloidal solution: amount of reducing agent and absorbing species in a solution, irradiation with electromagnetic radiation, temperature fluctuations and etc. The stability of a colloid results from the potential barrier that develops as a result of the competition between van der Waals attraction and Coulomb repulsion. Metal sols normally aggregate through two global (nanoparticle-concentration-dependent) mechanisms called cluster-particle aggregation and cluster-cluster aggregation. In the former, aggregates form primarily through the addition of single nanoparticles to a growing cluster. In the latter, clusters of all sizes can assimilate into larger clusters. An aggregating colloid can switch from one mechanism to the other as the number of particles becomes depleted [23].

The nanoparticles in a solution can be stabilized inserting nanoparticles in solid matrix or selecting the optimal formation conditions of the solution, which would prevent of further particle aggregation.

We have investigated the stability of our colloidal solution in time. We have chosen the solution that was boiled for 60 min according to the results described previously (highest absorption intensity, average value of FWHM). The solution was placed in dark when two different temperatures (19 °C and 11.8 °C) were applied. These two temperatures were chosen according to performed experiments [12, 13]. The stability of a colloidal solution was followed by UV-VIS spectroscopy. The spectra were taken after 24, 48, 96 and 120 hours has passed. In the earlier experiments it was observed, that the absorbance intensity of colloidal solution is increasing when it is left for some time [15].

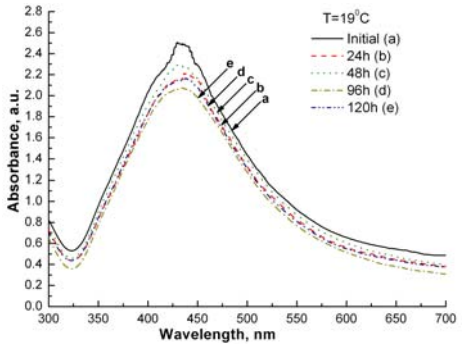

a

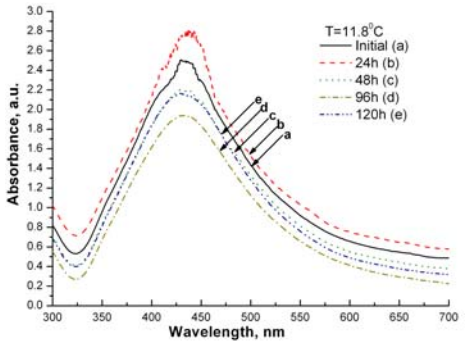

b

Fig. 6. Evolution of colloidal solution spectra after 24, 48, 96 and 120 h has passed after the synthesis: a – T = 19 °C, b – T = 11.8 °C

This time we have measured diluted colloidal solution because of high intensity, which can not be measured with the spectrophotometer. In all the measurements we have diluted colloidal solution with distilled water in ratio 1:1

(1 ml of colloidal solution and 1 ml of distilled water). The results are presented in Fig. 6. As one can see from the spectra, there is some variation in intensity versus time. For the case of colloidal solution left at room temperature the absorbance varies from 2 a.u to 2.6 a.u (see Fig. 6, a), and for lower temperature – from 1.9 a.u to 2.9 a.u (see Fig. 6, b).

Analysis of the peak position and FWHM was done approximating curve with Gaussian function. Results are presented in Fig. 7. Concerning the SPR position there is small variation in about 2 nm, this would lead to particle size change also in ~2 nm. Such small changes in particle size could not be observed due to reaching resolution limits of the spectrophotometer (1.4 nm). Evaluating the change of FWHM one could see that variation is in 5 nm, except one point when the colloid was left in temperature of 11.8 °C for the first 24 h. After this time the FWHM became narrower (also and SPR position was blue shifted). This could be explained by the abrupt end of the formation of nanoparticles after intensive heating and some destruction of present particles. If we would neglect this point one can see that all results obtained at different temperatures correlate with some uncertainties.

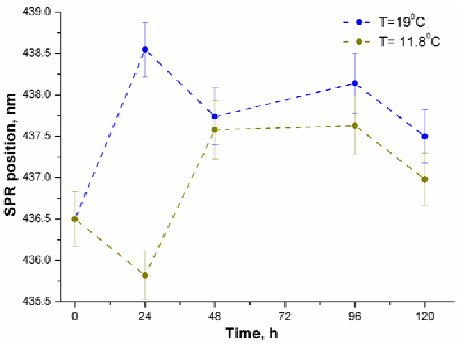

a

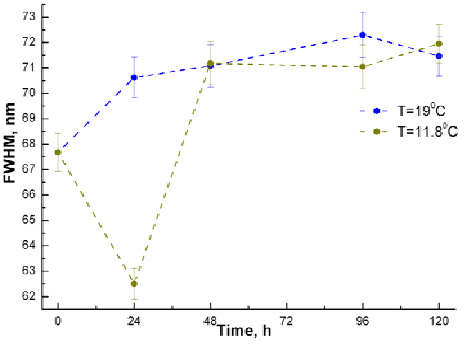

b

Fig. 7. Statistical parameters at different times after synthesis: a – SPR position, b – FWHM

4. CONCLUSIONS

We have shown that using chemical silver nanoparticle formation method (silver nitrate reduction with sodium citrate) we can achieve spherical nanoparticles with sizes in range of 45 nm – 80 nm determined from theoretical considerations (45 nm – 80 nm) and SEM analysis (45 nm – 50 nm). One can get differently sized nanoparticles at the steps of synthesis.

We have shown that colloidal solution boiled for 60 minutes is stable for 120 h at two different temperatures when no direct light is applied.

In order to get better size distribution correlation between different methods (theory and SEM), one could use other theoretical models (for example, discrete dipole approximation).

Acknowledgement

This work was supported by Lithuanian Science and Study Foundation, Ministry of Science and Education, NordForsk and COST action MP0803.

REFERENCES

1. **Kreibig, U., Vollmer, M.** Optical Properties of Metal Clusters. Springer, Berlin, 1995: pp. 203 – 275.
2. **Panigrahi, S., Praharaj, S., Basu, S., Ghosh, S. K., Jaha, S., Pande, S., Vo-Dinh, T., Jiang, H., Pal, T.** Self-assembly of Silver Nanoparticles: Synthesis, Stabilization, Optical Properties, and Application in Surface-enhanced Raman Scattering *The Journal of Physical Chemistry B* 110 (27) 2006: pp. 13436 – 13444.
3. **Lee, G.-J., Shin, S.-I., Kim, Y.-C., Oh, S.-G.** Preparation of Silver Nanorods through the Control of Temperature and pH of Reaction Medium *Materials Chemistry and Physics* 84 (2 – 3) 2004: pp. 197 – 204.
4. **Pastoriza-Santos, I., Liz-Marzán, L. M.** Colloidal Silver Nanoplates. State of the Art and Future Challenges *Journal of Materials Chemistry* 18 (15) 2008: pp. 1724 – 1737.
5. **Shirtcliffe, N., Nickel, U., Schneider, S.** Reproducible Preparation of Silver Sols with Small Particle Size Using Borohydride Reduction: for Use as Nuclei for Preparation of Larger Particles *Journal of Colloid and Interface Science* 211 (1) 1999: pp. 122 – 129.
6. **Prosyčevas, I., Juraitis, A., Puišo, J., Niaura, G., Guobienė, A., Tamulevičius, S., Balčaitis, G., Šileikaitė, A.** Synthesis and Characterization of Silver Nanoparticles *Proceedings of SPIE* 6596 2007: pp. 65960I (7 pages).
7. **Sondi, I., Goia, D. V., Matijević, E.** Preparation of Highly Concentrated Stable Dispersions of Uniform Silver Nanoparticles *Journal of Colloid and Interface Science* 260 (1) 2003: pp. 75 – 81.
8. **Pal, A., Pal, T.** Silver Nanoparticle Aggregate Formation by a Photochemical Method and Its Application to SERS Analysis *Journal of Raman Spectroscopy* 30 (3) 1999: pp. 199 – 204.
9. **Gutierez, M., Henglein, A.** Formation of Colloidal Silver by "Push-Pull" Reduction of Ag^{+} *The Journal of Physical Chemistry* 97 (44) 1993: pp. 11368 – 1 1370.
10. **Miranda, M. M.** SERS-active Ag/SiO_2 Colloids: Photoreduction Mechanism of the Silver Ions and Catalytic Activity of the Colloidal Nanoparticles *Journal of Raman Spectroscopy* 35 (10) 2004: pp. 839 – 842.
11. **Abu Hatab, N. A., Oran, J. M., Sepaniak, M. J.** Surface-Enhanced Raman Spectroscopy Substrates Created via Electron Beam Lithography and Nanotransfer Printing, American Chemical Society *ACS NANO* 2 (2) 2008: pp. 377 – 385.
12. **Šileikaitė, A., Puišo, J., Prosyčevas, I., Guobienė, A., Tamulevičius, S., Tamulevičius, T., Janušas, G.** Polymer Diffraction Gratings Modified with Silver Nanoparticles *Materials Science* (*Medžiagotyra*) 13 (4) 2007: pp. 273 – 277.

13. **Šileikaitė, A., Tamulevičius, T., Tamulevičius, S., Andrulevičius, M., Puišo, J., Guobienė, A., Prosyčevas, I., Madsen, M., Maibohm, C., Rubahn, H.-G.** Periodic Structures Modified with Silver Nanoparticles for Novel Plasmonic Application *Proceedings of SPIE* 6988, 69881Q (April, 23, 2008) (published online, http://spiedigitallibrary.aip.org).
14. **Lee, P. C., Meisel, D.** Adsorption and Surface – Enhanced Raman of Dyes on Silver and Gold Sols *Journal of Physical Chemistry* 86 1982: pp. 3391 – 3395.
15. **Šileikaitė, A., Prosyčevas, I., Puišo, J., Juraitis, A., Guobienė, A.** Analysis of Silver Nanoparticles Produced by Chemical Reduction of Silver Salt Solution *Materials Science* (*Medžiagotyra*) 12 (4) 2006: pp. 287 – 291.
16. http://www.wavemetrics.com/ (status of 2008-07-20).
17. The "ImageJ" Software is Available at http://rsb.info.nih.gov/ij/ (status of 2008-07-20).
18. **Krylova, G., Eremenko, A., Smirnova, N., Eustis, S.** Structure and Spectra of Photochemically Obtained Nanosized Silver Particles in Presence of Modified Porous Silica *International Journal of Photoenergy* 7 (4) 2005 pp. 193 – 198.
19. **Velikov, K. P., Zegers, G. E., Blaaderen, A.** Synthesis and Characterization of Large Colloidal Silver Particles *Langmuir* 19 (4) 2003: pp. 1384 – 1389
20. **Evanoff, D. D., Chumanov, G.** Size-controlled Synthesis of Nanoparticles. 1. "Silver-Only" Aqueous Suspensions via Hydrogen Reduction *Journal of Physical Chemistry B* 108 (37) 2004: pp. 13948 – 13956
21. **Ershov, B. G., Janata, E., Henglein, A., Fojtik, A.** Silver Atoms and Clusters in Aqueous Solution: Absorption Spectra and the Particle Growth in the Absence of Stabilizing Ag^+ Ions *Journal of Physical Chemistry* 97 (18) 1993: pp. 4589 – 4594.
22. The "MiePlot" Software is available from Philip Laven, available at www.philiplaven.com/mieplot.htm
23. **Moskovits, M., Vlckova, B.** Adsorbate-induced Silver Nanoparticle Aggregation Kinetics *The Journal of Physical Chemistry B* 109 (31) 2005: pp. 14755 – 14758.

Presented at the 17th International Conference "Materials Engineering'2008"
(*Kaunas, Lithuania, November 06 – 07, 2008*)